Automatic 3D Boresight and Latency Estimation of IMU and Multi-Beam Echo Sounder Systems*

N. SEUBE[1] , S.LEVILLY[2] and R. KEYETIEU-NLOWE[2]
[1]CIDCO, Rimouski, QC
CANADA
[2]ENSTA Bretagne, Brest
FRANCE

Abstract

This paper present some methods for automatic boresight and latency calibration for Multi Beam Echo Sounders and Inertial Measurement Units. The approach is based on the analysis of overlapping data and the resolution of surface matching problems. Surface patches and data are selected in order to guarantee the observability of the effet of boresight and latency. These methods are intended to replace the classical patch-test by full automatic 3D calibration methods.

Introduction

Calibration of Muti Beam Echo Sounder (MBES) systems is an important part of hydrographic survey systems mobilisation and requires a special attention in order to avoid the presence of systematic errors. This paper focuses on MBES-IMU boresight (i.e. the misalignement angle between the MBES frame and the IMU frame) and latency (i.e. the time delay between the physical IMU attitude angle measurement and the MBES measurement). The objective of the methods we describe here is to reduce time and effort devoted to boresight and latency estimtates and to provide quality control report after calibration.

We first consider the problem of boresight calibration of a classical swath system, composed by a Multi-Beam Echo Sounder (MBES), an Inertial Measurement Unit (IMU) and a positioning system (GNSS receiver). From MBES, IMU and GNSS source data one can determine a sounding 3D position though the following georeferencing model:

$$X_n(t) = P_n(t) + C^n_{bI}(t - dt)[C^{bI}_{bS}\vec{r}_{bS}(t) + \vec{a}_{bI}] \qquad (1)$$

*This work has been partially funded under a research contract with FUGRO BV, FUGRO INTERSITE, FUGRO Geo-Consulting.

where $X_n = (x, y, z)_n$ is the position of a sounding in a navigation frame *(n)* (which can be a local geodetic frame), P_n is the position delivered by the GNSS receiver in frame *(n)*, C^n_{bI} is the coordinate transformation from the IMU body frame to the navigation frame (which can be parametrized using Euler angles (φ, θ, ψ), denoting roll, pitch and yaw), the MBES return r_{bS}, coordinated in the MBES frame *(bS)*, the lever-arm vector (difference between the MBES acoustic center and the positioning reference point) coordinated in the IMU frame $\vec{a}_{bI}$ and the boresight coordinate transformation C^{bI}_{bS}.

In equation (1), t denotes the reference time from the GNSS receiver, which is supposed to be propagated withini the system through a time tagging procedure, and dt denotes the potential latency between the MBES and the IMU.

The dependency of the calibration parameters on soundings spatial referencing is described by equation (1), among them are:

- dt, the latency between the IMU and the MBES system (it is to be noticed that in most modern hydrographic systems, latency between GNSS and the MBES impact can be considered as negligible, but latency between the MBES and IMU may not be [Seube(2012)];
- C^{bI}_{bS}, the boresight coordinate transformation;
- $\vec{a}_{bI}$, the lever-arms which may be affected by static measurement errors, coordinate transformation errors from the measurement frame to the IMU frame, and in some cases, time-varying (for large ships for instance);
- The MBES range and beam launch angles, affecting the term $\vec{r}_{bS}$.

This article will focus on the estimation of both boresight coordinate transformation C^{bI}_{bS} and latency dt.

1 Boresight calibration

Boresight calibration consists in determining the coordinate transformation C^{bI}_{bS} from overlapping swath lines. In hydrographic surveying, the most classical method to determine this matrix is the so-called "patch-test" (also called the "Swath Alignment Method"), introduced at the end of the 80' [Herlihy et al. (1989), Hammack et al. (1998), Godin, 1998] which principle is recalled here.

Assumptions are made that position, attitude, heave, tide and (Sound Speed Profiles) SSP are known and applied within the MBES (or within the acquisition system) and that each sensor provides measurements within its own reference frame and time-tag.

The patch-test decouples the three boresight angles estimation problem, starting with roll , followed by pitch, and then yaw. For roll boresight calibration, a flat bottom, surveyed in opposite direction is used, since the roll boresight $\delta\varphi$ effect can be easily characterized. In practical situations, the roll boresight precision and accuracy generally far beyond the precision achieved by the IMU. Pitch boresight calibration uses nadir data from two opposite lines over a slope. Figure 1 illustrates the effect of a pitch boresight $\delta\theta$ over a regular slope, followed by a flat terrain. Yaw boresight calibration is done by surveying two parallel lines in the same direction over a regular slope.

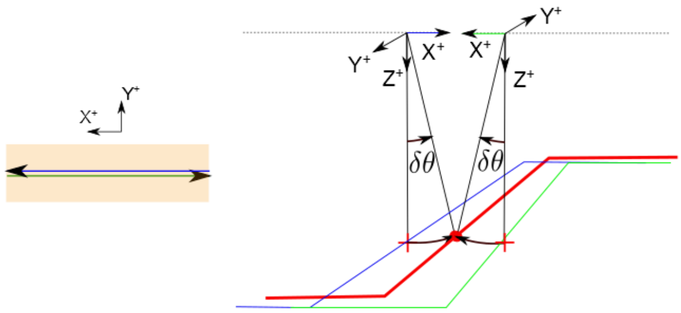

Figure 1: Effect of pitch boresight on two opposite lines over a slope.

In most boresight calculation implementations, the estimation is done through two steps:

1. The user selects a subset of the data set from overlapping areas;
2. In sweeping the possible boresight values, one re-computes corrected data according to the spatial referencing equation (1), and builds a digital terrain model from the overlapping data sets. Then, one compares the discrepancy between those models, and chooses the lowest one.

We observe that through this classical patch-tes procedure,

- the choice of the data analysis area influences the boresight estimation and is left to the user;
- the method cannot be generalized to a 3D analysis, as the sweeping process in 3D would be time consuming;
- no estimation of the boresight angle precision can be provided.

The effect of boresight on survey data is rather complex, with each swath being modified according to the local seafloor morphology which determines the beams grazing angles and therefore impacts the error between the actual and assumed sounding. Indeed, a boresight error acts as a rotation around the acoustic center of the MBES which position varies in time. It is therefore impossible to model the effect of the boresight angle over a global surface by a simple geometric transformation like a similarity transformation for instance. In Fig. 1, the nadir beams are plotted for two opposite survey lines over a slope and flat areas. From this figure, it can be easily seen that it is impossible to deduce the actual sea floor from the assumed seafloors by a simple geometric transformation. From this remark, we deduce that boresight must be determined from a local analysis.

Another problem is the coupling between roll, pitch and yaw angles, which can be understood from the geo-referencing equation (1). Indeed, entries of the coordinate transformation matrix (in NED convention) $C_{bS}^{bI} = C_3(\delta\psi)C_2(\delta\theta)C_1(\delta\varphi)$ depend on the three boresight angles, which means that they contribute to each swath return distortion by coupling. We have seen that the classical patch-test method first determines the roll, then the pitch and finally, the yaw boresight. This implies that the roll boresight is determined with uncorrected pitch and yaw. In case of a non-perfectly flat sea-floor, pitch and yaw actually contribute to the MBES swath return distortion. This effect of boresight angles cross-talk has the following consequence. The determination of roll is biased by the absence of knowledge of pitch and yaw which impact data used for roll calibration over non-perfectly flat local surfaces. After roll determination, the pitch is estimated using nadir data over a slope, therefore without critical impact of roll boresight error. Yaw estimation maybe biased by the residual roll and pitch errors since it uses full swath data over a slope. It is actually the case in practice, the yaw boresight remains the most difficult to estimate, which is due to the fact the patch-test procedure uses biased data and makes inappropriate assumptions.

In summary,

1. Each patch of non-planar surfaces is distorted by "local" rotations which depends on swath attitude angle and therefore on local grazing angles;
2. Boresight decoupling assumptions are not valid, since each boresight angle which has not yet been corrected may distort a non-planar surface.

Some aletnative methods to the classical patch test have been intensively studied for Airborne LiDAR Systems (ALS) applications [Morin and Naser El-Sheimy(2002)], [Filin(2003)], [Glennie(2007)]. Among the approaches that have been developped, the most promising seems to be the one based on local surface patch normal fitting [Skaloud and Litchi(2006)] [Skaloud(2007)]. Generally, these methods make the assumption that local planr surface patch can be found, which may not be appropriate for hydrographic surveying. Therefore, a significant adaptation of these methods to calibration overr natural surfaces have to be done.

2 Latency calibration

The latency we consider here is between the IMU and the MBES. A time delay may have a significant impact on the data set, creating oscillations on the outer beams of the MBES, as shown in figure (2). The MBES/INS latency (denoted by dt in equation (1) has not yet been studied, and no clear methodology is available for its automatic computation from source data. However, this latency maybe be an important source of error and may occur in case of unexpected failure of the time-tagging electronic implementation, as explained in [Hughes Clarke, J. (2003)].

From a hardware point of view, latency may be reduced if a time-tagging strategy is properly implemented. Modern time-tagging implementations make use of the GNSS receiver computed time as a reference time for all sensors. The time-tagging signal (called PPS, Pulse Per Second) and a time message are distributed to the

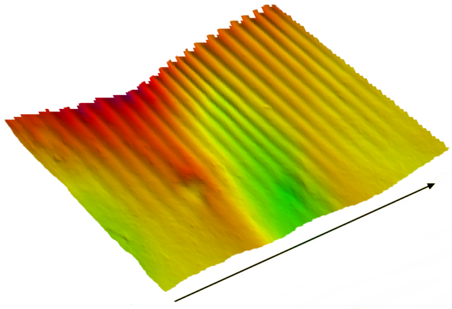

Figure 2: Example of latency effect on survey data taken from a survey vessel having fast roll motion dynamics.

IMU and MBES, allowing them to synchronize their own clock and to time-tag output data before sending them through a data link. This model is known as the "distributed time and message" approach (See [Calder et al. (2007)]). However, single oscillators models (i.e. centralized time-tagging without propagation of PPS and time message) may still be implemented in some hydrographic systems.

Even if distributed time and message type of time-tagging reduces dramatically the latency between the different hydrographic sensors outputs, one may observe that the total latency (aggregate time between the physical measurement, the output of each sensor, transmission time, buffering time, acquisition, time matching with other data for geo-referencing purposes) may not be negligible.

In [Seube(2012)], the *total* latency of a classical distributed time and message time-tagging systems have been accurately estimated for a LiDAR and IMU system through a laboratory test. However, this preocedure requires the LiDAR to be mounted on the same mechanical bracket than the INS, which is generally impossible for MBES system. Here again, we nee to adapt methods that have been develop for LiDAR application to on-the-field calibration procedure.

3 Automatic MBES-IMU Boresight Calibration

The methods we propose are based on the following:

- The use of a spatial reference model taking into account boresight angles, lever-arms and other source data provided by the survey sensor suite (positioning, IMU, MBES);
- The definition of an observation equation expressing the fact that overlapping data should coincide;
- The definition of an automatic data selection process which returns appropriate overlapping subsets;
- Adjustment methods which provide numerical estimation of the boresight angles;

- Statistical analysis tools that provide external and internal reliability of the estimation process, and returns boresight angle precision.

It has been mentioned that a global surface distortion due to boresight cannot be represented by a simple geometrical transformation like a similarity transformation for example. Indeed, from Fig. 1, one can readily see that both assumed (i.e. distorted) profiles (in green and blue) cannot be transformed into the actual profile represented in red. This simple observation enables us to classify several types of boresight calibration and estimation methods:

- *Rigorous*, methods and estimation procedures which estimate the boresight coordinate transformation from elementary sounding (e.g., points) or a subset of sounding from the same swaths. Indeed, these objects are submitted to a coordinate transformation which belongs to the class of transformations we are looking for.
- *Semi-Rigorous*, methods that estimate the boresight coordinate transformation using local overlapping surfaces patches.
- *Non-Rigorous*, all other methods.

We shall say that a boresight calibration method is a decoupling method if it ignores the coupling between roll, pitch and yaw. From this classification, we can say for example that the classical patch-test is a rigorous decoupling method. Referring to normal fitting methods, widely used in LiDAR applications, we can say that they are actually semi-rigorous, but non-decoupling: Indeed, these methods estimate normal vectors to local surfaces patches constructed from overlapping data sets (i.e., they are semi-rigorous) and they adjust in 3D the boresight angles in order to fit these normal vectors (i.e., they are non-decoupling methods).

3.1 Working Limits

Our aim is to design a 3D rigorous method, which can be easily automated by analyzing relevant overlapping swath data, and which provides boresight angle precision estimation. We present here a method which seems promising from preliminary experimental results.

Let us suppose that the boresight calibration data subset is a set of overlapping swaths over a given area. This area needs to be defined such that all boresight angles produce significant (i.e; observable) sounding errors. One should avoid for instance flat areas (for which pitch and yaw are not observable) and prefer slopes. One should also avoid areas containing edges (like wrecks for instance), since the sampling effect between overlapping datasets may transfer into boresight bias.

From the spatial referencing equation (1), assuming that latency is corrected (e.g. known from either a systemic analysis or estimated), we have:

$$X_n(t) = P_n(t) + C_{bI}^n(t)[C_{bS}^{bI}\vec{r}_{bS}(t) + \vec{a}_{bI}] \tag{2}$$

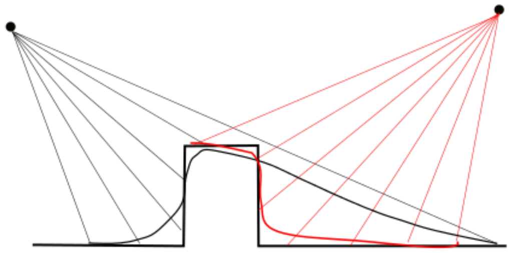

Figure 3: Fake boresight error from overlapping data over an edge, due to different point of view and space sampling effect.

For the sake of simplicity, we suppose that IMU data $C_{bI}^n(t)$ are not biased (i.e., the IMU is properly aligned with the local geodetic frame) and that MBES returns are not subject to launch angle and range bias. This is actually the case whenever the IMU is properly calibrated and aligned, sound speed profiles are known without uncertainty, and the surface sound velocity is correctly measured and fed into the MBES.

Let us consider a cell from a grid defined over overlapping swaths. Within every cell, we express the fact that if all points, corrected with appropriate boresight and lever-arm values lie on a given quadratic surface, then the boresight and lever-arm errors should be zero (see Fig. 4 below). From a practical point of view, if the grazing angles of the MBES swaths cover a sufficiently wide interval (i.e., if the calibration lines are run over a slope from distinct points of views), we should be able to estimate the boresight angles. In other words, the boresight angles should be observable.

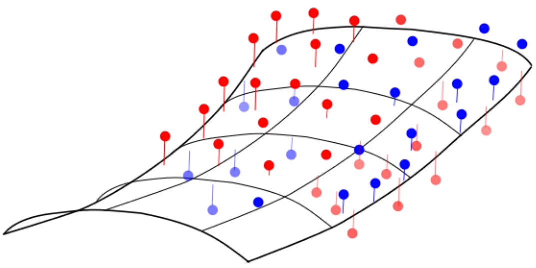

Figure 4: Before boresight calibration, soundings from two overlapping swaths generally don't fit . In this example, the two point clouds do not match with any quadratic surface. In our approach, the quadratic surface and the boresight angles are adjusted in order to fit the overlapping point clouds.

3.2 Observation Equation

We detail now how this problem can be expressed as an iterative least squares problem, and how the sounding uncertainties can be propagated through this least squares problem in order to get estimates of both boresight and lever-arm precision.

Let us denote by $\vec{p}$, the vector of (unknown) parameters defining a quadratic surface $S(\vec{p}; x, y, z) = 0$, and by $\vec{\chi} = (\delta\varphi, \delta\theta, \delta\psi)$, the vector of unknown boresight angles. $\vec{p}$ can be chosen to be a 6 dimensional vector, and $\vec{\chi}$ is a 3 dimensional vector. Using this notation we can write equation (2) as:

$$X_n = f(\vec{\chi}; P_n(t), C_{bI}^n(t), \vec{r}_{bS}(t), \vec{a}_{bI}) \tag{3}$$

Where $P_n(t), C_{bI}^n(t), \vec{r}_{bS}(t)$ are here considered as external data depending on each sounding measured at time t. The criterion we use to determine both $\vec{p}$ and $\vec{\chi}$ is expressed in the Eq. (4).

$$S(\vec{p}; f(\vec{\chi}; P_n(t), C_{bI}^n(t), \vec{r}_{bS}(t), \vec{a}_{bI})) = 0 \tag{4}$$

Equation (4) express the fact that the point $X_n(t)$ lies on a given quadratic surface. Let us now consider the collection of conditions, for all overlapping points of a given grid, defined on the horizontal plane. After linearization, this system, can be written as an optimization problem that can be solved by an iterative least square procedure and enables both external and internal reliability analysis.

4 Numericals Results

We present some results, obtained from the application of the method presented above from calibration lines performed with an hydrographic system composed of an R2SONIC 2022, an IXBLUE OCTANS4, and a MAGELLAN proflex500 GNSS receiver. The data acquisition software used was QINSy. These tests have been conducted by using the ENSTA Bretagne hydrographic survey vessel over a slope located in the Brest harbor.

Let us first mention that the geometry of line and overlaps used by our method is different from the classical patch-test method. Indeed, we need to guarantee boresight angle observability, which can be achieved only with a set of swaths obtained from significantly different points of view of the same area. Therefore, a set of crossing lines over a slope has been surveyed. In order to compare our approach with the patch-test, we also performed patch test lines (over flat surfaces for roll, and the same slope for pitch and heading), and estimated calibration parameters with classical software tools. Table 1 presents the values of the boresight angles found by Automatic Boresight Estimation (ABE) and the classical patch-test.
As a measure of the precision of the bathymetric surface built with a given boresight value, we use the following process: For each cell of a grid, we fit a plane by total least square (TLS) and use the orthogonal error of the point cloud which is given by the lowest singular value computed by the TLS. The advantage of this method with

Table 1: Calibration Numerical Results in the Brest Harbor

Boresight Angles [°]	Roll ($\delta\varphi$)	STD	Pitch ($\delta\theta$)	STD	Yaw ($\delta\psi$)	STD
Patch-test	0.62	?	1.64	?	1.88	?
ABE	0.679	0.006	1.657	0,002	1.995	0.03

respect to the classical standard deviation map is to cancel out the effect of local slopes.

Figure 5 shows the histogram of the orthogonal error (i.e., seabed width standard deviation) for both our approach and a classical patch test. Figure 6 presents the chart results obtained using the calibration results of the Table 1.

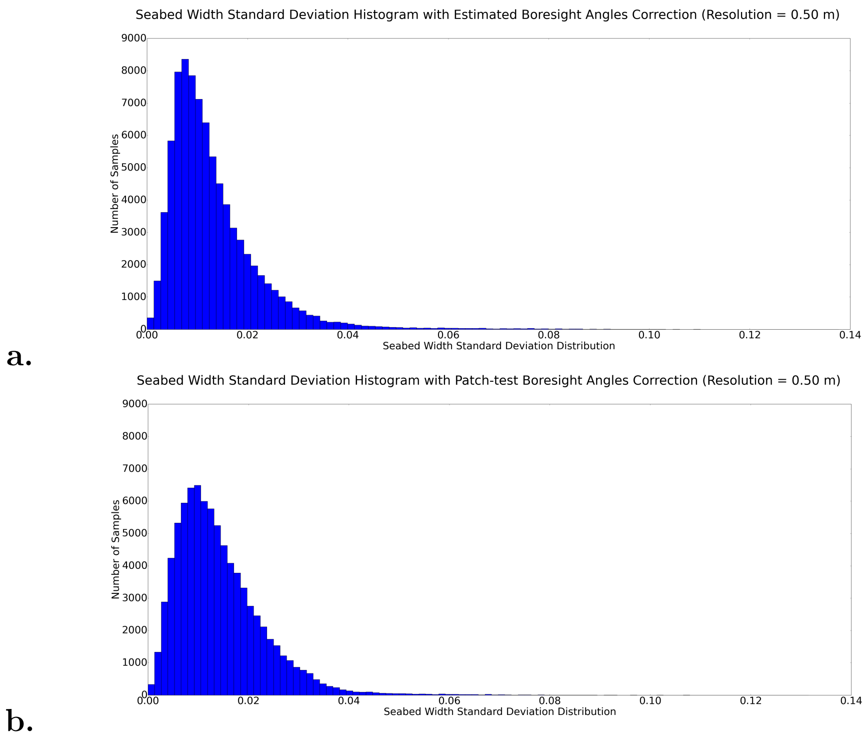

Figure 5: From the two histograms, one can see that the automatic boresight method (**a**) provides a better global fit of overlapping data. Indeed the plot shows number or samples versus the adjustment error. **a** seabed width standard deviation histogram with estimated boresight angles correction. **b** seabed width standard deviation histogram with Patch-test boresight angles correction.

By observing figure 6 one can see that the automatic boresight calibration method is performing better. **a** seabed width standard deviation with the estimated boresight angles correction on a flat area. In addition, as shown in table 1, the additional added value of this method is to provide boresight angle precision based on a statistical analysis.

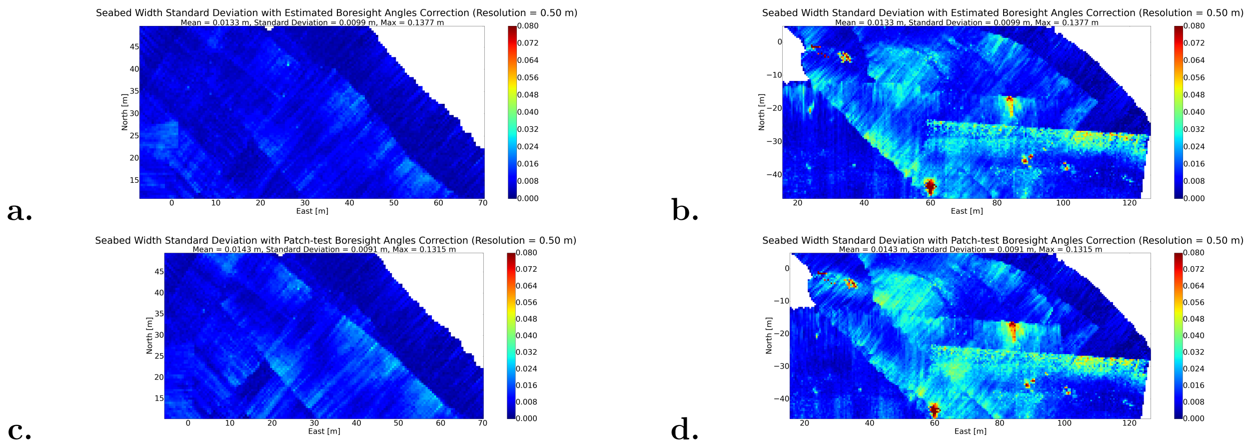

Figure 6: Global data set precision estimation, for the boresight estimated by our automatic method (top **a** and **b**) and a classical patch test (bottom **c** and **d**). **b** seabed width standard deviation with the estimated boresight angles correction on a mix flat/slope area. **c** seabed width standard deviation with the Patch-test boresight angles correction on a flat area. **d** seabed width standard deviation with the Patch-test boresight angles correction on a mix flat/slope area.

5 Automatic latency calibration

The principle of the method we propose is based on the following idea: The effect of latency can be observed on MBES swath measured at high attitude velocities and small attitude acceleration, thus for calibration purposes, we should only select these data in order to actually observe the latency effect. We then write an observation equation which translates the fact that over small surface patches, the geo-referenced data should be smooth, which can be guaranteed by forcing the data to belong to a given parametric surface.

If we consider MBES swath data with a small attitude acceleration, we can write:

$$\begin{aligned} C^n_{bI}(t-dt) &= C^n_{bI}(t) - dt\, \dot{C^n_{bI}}(t) && (5)\\ &= C^n_{bI}(t) - dt\, C^n_{bI}(t)\, \Omega^{bI}_{n/bI}(t) && (6)\\ &= C^n_{bI}(t)\, (Id - dt\, \Omega^{bI}_{n/bI}(t)) && (7) \end{aligned}$$

where $\Omega^{bI}_{n/bI}(t)$ is the skew-symetric matrix associated to the angular velocity vector $\omega^{bI}_{n/bI}(t)$. Thus, the geo-referencing equation becomes:

$$X_n(t) = P_n(t) + C^n_{bI}(t)\, (Id - dt\, \Omega^{bI}_{n/bI}(t))\, (C^{bI}_{bS}\, r_{bS}(t) + a_{bI}) \quad (8)$$

We need first to estimate $\Omega^{bI}_{n/bI}(t)$ (done by the application of a Kalman filter on the attitude data)[1]. Knowing this, translate the fact that all geo-referenced data should lie on the same smooth surface in the following observation equation:

[1]Note that this step could be avoided if the acquisition system was providing angular rates, which are directly available from the IMU.

$$z_n = A\, x_n^2 + B\, y_n^2 + C\, x_n\, y_n + D\, x_n + E\, y_n + F \tag{9}$$

where $A, B, \ldots F$ are unknown parameters modeling a small quadratic surface patch, and $(x_n, y_n, z_n) = X_n$, which depends on the latency parameter dt. Note that all other parameters from equation (8) are either measurements or computed values, like $\Omega_{n/bI}^{bI}(t)$.

Our problem is therefore under the form of a non linear optimization problem that we can solve by an Iterative Least Square procedure. Note that ILS interest is to provide statistical estimation of the estimated parameters covariances, here an estimation of the estimated latency variance.

In order to validate this approach, we simulated a MBES data set comprising IMU, positioning, and MBES swath returns over ramdom terrains (results are here presented in the case of a slope). The simulated attitude (pitch, roll and yaw) data are plotted on figure (7). A fake latency of 10ms has been added to desynchronize the MBES data from IMU data. Our aim is from randomly generated MBES data to determine the accuracy of the estimation and its precision.

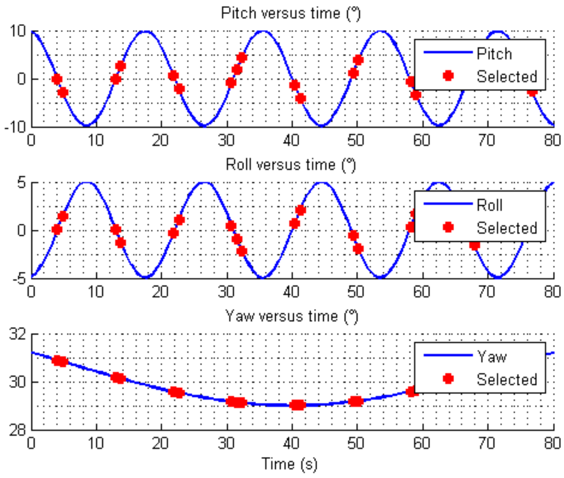

Figure 7: Red dots are te selected attitude points for latency calibration, corresponding to maximum angular velocity from their Kalman estimated

In figure (7) we plotted the data set before latency estimation and correction, and after latency estimation and correction. One can check that from these plots, the data set seems more consistent. However, our latency estimation method being not based on the comparison of two data sets (one before and one after correction), we can derive a estimation of the latency accuracy and precision. Accuracy can be here provided as we introduced a priori know fake latencies. Precision comes from a statistical analysis of the ILS solution. From a series of numerical simulations we observed that:

- The accuracy of the estimation is independent of the "fake" latency added to the system, and is less than 1ms;

- The precision of the estimated latency is 0,4 ms.

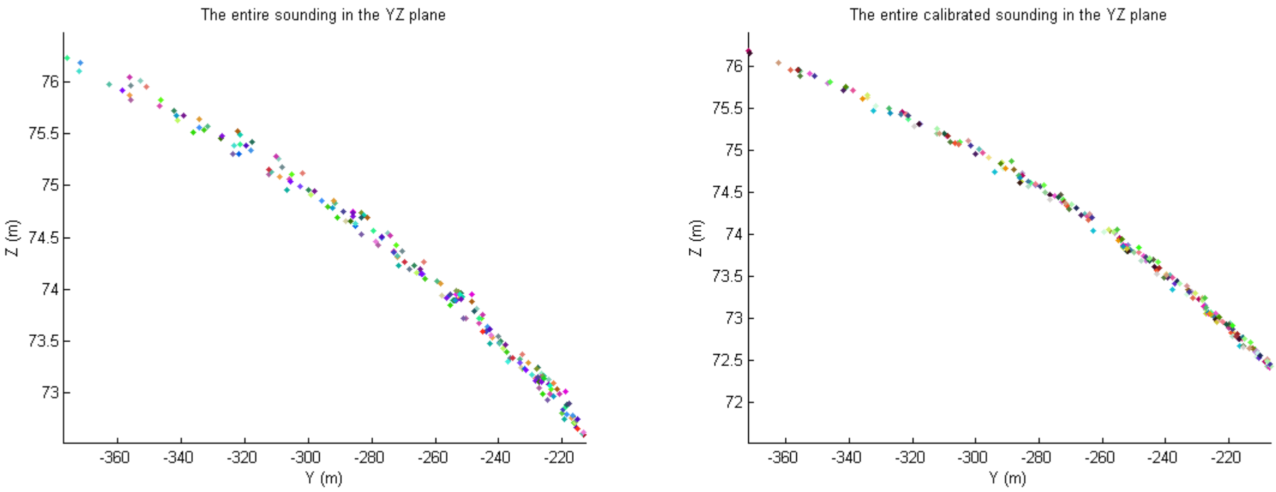

Figure 8: On the left, soundings plotted on the (East,Down) plane before correction from estimated latency, on the right, sounding corrected from estimated latency.

These preliminary results shows that latency calibration can be performed from MBES data by forcing the smoothness of the resulting dataset. This method do not require any overlapping data. The 0,4ms precision is consistent with most hydrographic requirements.

The robustness of the latency estimation with regards to Surface Sound Speed (SSS) variations in the presence of significant roll variations and heave (as mentioned in [Hughes Clarke, J. (2003)]) has also been tested. Indeed, these errors produce artifact which are "visually" comparable to latency effects. The latency accuracy remains under 1ms even in the presence of hard SSS variations (about 20m/s at 0.4m depth) and roll variations. The latency precision remains under 1ms which is still acceptable.

This method can therefore be envisioned to calibrate and even monitor the MBES system latency in order to prevent from PPS time and message synchonization implementation failures.

6 Conclusion

The automated boresight calibration procedure introduced in this paper provides promising preliminary results. The use of an observation equation and least-squares optimization method was used to solve the full 3D boresight angle estimation problem from overlapping source data. Furthermore, statistical analysis enables us to derive calibration reports under the form of boresight angle estimated precision. All these aspects give the essential information (value, precision, internal and external reliability) which should be part of any calibration report. Moreover, this automatic procedure allows the hydrographer to save survey and processing time. The results presented need to be confirmed by other tests with different systems and other survey areas.

Latency estimation from MBES system data is possible through the use of appropriate data selection and the numerical resolution of a surface matching optimization problem. The method exisbits a good behvior on simulated data and is currently under further investigation on real datasets comming from different MBES systems.

References

[Barber and Mills(2006)] Barber, D., Mills, J., 2006. Geometric validation of ground-based mobile laser scanning system. ISPRS Journal of Photogrammetry & Remote Sensing 68, 123–141.

[Burman (2000)] Burman, H., 2000. Calibration and orientation of airborne image and laser scanner data using GPS and INS PhD Dissertation, Royal Institute of Technology Department of Geodesy and Photogrammetry, Stockholm, Sweden, April 2000

[Calder et al. (2007)] Calder, B.R., Brennan,R.T, Malzone, C., Marcus, J., Canter, P., 2007 Application of High-Precision Timing to Distributed Survey Systems , Proc. of the US-Hydro Conference.

[Eisenberg et al. (2011)] Eisenberg, J., Davidson, M., Beaudoin, J?, Brodet, S., Rethinking the Patch Test for Phase Measuring Bathymetric Sonars, Proceedings: US Hydrographic Conference, Tampa, FL, 25-28 April 2011

[Filin(2003)] Filin, S., 2003. Recovery of systematic biases in laser altimetry data using natural surfaces. Photogrammetric Engineering & Remote Sensing 69, 1235–1242.

[Filin and Vosselman(2004)] Filin, S., Vosselman, G., 2004. Adjustment of airborne laser altimetry strips. In: ISPRS Congress Istanbul, Proceedings of Commission III.

[Gaumet(2013)] Gaumet, M., 2013. Automatic Calibration Methods, Master thesis report, CARIS/ENSTA Bretagne, Sept 2013.

[Glennie(2007)] Glennie, C., 2007. Rigorous 3d error analysis of kinematic scanning lidar systems. Journal of Applied Geodesy 1, 147–157.

[Godin, 1998] Godin, A. (1998), The Calibration of Shallow Water Multibeam Echo-Sounding Systems, M.Eng. Report, Department of Geodesy and Geomatics Engineering Technical Report No. 190, University of New Brunswick, Fredericton, New Brunswick, Canada, 182 pp.

[Gruen and Beyer(2001)] Gruen, A., Beyer, H., 2001. Calibration and Oritentations in Computer Vision. Springer, Ch. System Calibration through Self-Calibration., pp. 163–193.

[Habib et al.(2010)] Habib, A., Bang, K., Kersting, A., Chow, J., 2010. Alternative methodologies for lidar system calibration. Remote Sensing 2, 874–907.

[Habib et al.(2010)] Habib, A., Kersting, A., Bang, K., 2010. Impact of LiDAR system calibration on the relative and absolute accuracy of the adjusted point cloud. Proc. Int. Calibration Orient. Workshop EuroCOW, pp.1 -6 2010.

[Hammack et al. (1998)] Hammack, J.A., Fabre, D.H., Hughes Clarke, J.E. and Reed, B., 1998, Hydrographic multibeam processing system (HMPS) swath alignment tool: Proceedings Canadian Hydrographic Conference 1998, Victoria, p. 157-167.

[Hebel et al. (2012)] Hebl, M. and Uwe, S., Simultaneous Calibration of ALS Systems and Alignment of Multiview LiDAR Scans of Urban Areas, IEEE Transactions on Geoscience and Remote Sensing, Vol. 50, No. 6, June 2012, pp. 2364-2379.

[Herlihy et al. (1989)] Herlihy, D.R., B.F. Hillard, and T.D. Rulon (1989), National Oceanic and Atmospheric Administration Sea Beam System "Patch Test", International Hydrographic Review 66(2): 119- 139.

[Hughes Clarke, J. (2003)] Hughes Clarke, J., (2003), Dynamic Motion Residuals in Swath Sonar Data : Ironing out the Creases, International Hydrographic Review

[Kumari et al.(2011)] Kumari, P., Carter, W. E., Shrestha, R. L., 2011. Adjustment of systematic errors in als data through surface matching. Advances in Space research 47, 1851–1864.

[Le Scouarnec et al.(2013)] Le Scouarnec, R., Touzé, T. Lacambre, J.-B., Seube, N. , 2013. A positioning free calibration method for mobile laser scanning applications. ISPRS Annals of the ISPRS and SIS, Vol II-5/W2, 2013.

[Mettenleiter et al.(2008)] Mettenleiter, M., Oberteiber, N., Hartl, F., Ehm, M., Baur, J., Frohlich, C., 2008. 3d laser scanner as part of kinematic measurement system. In: Internation Conference on Machine Contol & Guidance.

[Morin and Naser El-Sheimy(2002)] Morin, K., Naser El-Sheimy, N., 2002. Postmission adjustment methods of airborne laser scanning data. In: FIG XXII Int. Congress, Washington DC.

[Schenk(2001)] Schenk, T., 2001. Modeling and analyzing systematic errors of airborne laser scanners. Tech. rep., Department of Civil and Environmental Engineering

[Seube(2012)] Seube, N, Picard, A. and Rondeau, M., 2012. A simple method to recover the latency time of tactical grade IMU systems, ISPRS Journal of Photogrammetry and Remote Sensing 74 (2012) 85-89

[Skaloud(2006)] Skaloud, J., 2006. Reliability of direct georeferencing: Phase 0. Tech. rep., Euro SDR commission 1: sensors, primary data, acquisition and georeferencing.

[Skaloud and Litchi(2006)] Skaloud, J., Litchi, D., 2006. Rigorous approach to boresight self-calibration in airborne laser scanning. ISPRS Journal of Photogrammetry & remote Sensing 61, 47–59.

[Skaloud(2007)] Skaloud, J., Shaer, P., 2006. Towards automated LiDAR boresight self-calibration. Proc. 5th Int. Symp. Mobile Mapping Technol., May 29-31, 2007.

[Smith (1991)] Smith, F.W., (1991), Estimating array misalignment errors in the Sea Beam sonar system: NOAA SBIR phase II final report, Contract 50-DKNA-9-00144.

[Weathon et al. (1988)] Wheaton, G.E. (1988), "Patch Test", A System Check For Multibeam Survey Systems, In Proc. Third Biennial U.S. Hydrographic Conference, April 1988.